Available online at www.sciencedirect.com

SciVerse ScienceDirect

Ceramics International 38 (2012) 5223–5229

CERAMICS INTERNATIONAL

www.elsevier.com/locate/ceramint

Macro/micro structure dependence of mechanical strength of low temperature sintered silicon carbide ceramic foams

Fei Chen [a,1], Ying Yang [a,b], Qiang Shen [a,*], Lianmeng Zhang [a]

[a] State Key Lab of Advanced Technology for Materials Synthesis and Processing, Wuhan University of Technology, Wuhan 430070, PR China
[b] Department of Chemical and Materials Engineering, University of Alberta, Alberta T6G 2V4, Canada

Received 27 February 2012; received in revised form 11 March 2012; accepted 11 March 2012
Available online 17 March 2012

Abstract

SiC foams with high strength were prepared by polymer replica technique, including coating with SiC slurry (using Al_2O_3 and Y_2O_3 as the sintering additives) and polymer replica removal. The results suggest that the macro porous structure, including the pore size and the strut diameter, could be controlled by choosing different polymer sponge templates with the different PPI (pores per inch) values and slurry coating times. Liquid phase sintering plays a significant role in the low temperature densification of the cell struts of SiC foams. The compressive strength increased significantly with the tendency of cell strut densification. SiC ceramic foams with PPI value of 20, porosity of 77%, highly densified strut microstructure and maximum compressive strength of 2.48 MPa were obtained at 1700 °C with SiC as the main phase.

Keywords: A. Sintering; C. Mechanical properties; D. SiC; Polymer replica technique

1. Introduction

Silicon carbide (SiC) foam is one of the most promising candidates for applications in the filtration of molten metals, industrial hot gas filters, catalyst supports, etc., due to its unique structures with extremely interconnected cell and high surface area, and excellent physical properties such as corrosion resistance, low thermal conductivity and low thermal expansion coefficient [1–3]. Several processing methods, assisted by pore-forming agent, polymer template and natural template, have been developed in order to achieve the enhanced features [2,3]. Among them, polymer replica technique is quite attractive for the macro cells of 200 μm–3 mm, which supplies a simple fabrication process for industry production. However, the high porosity generally results in the low mechanical strength due to the weakness of the foam struts, which limits their application in energy and environment fields.

The major reasons responsible for the weakness of the foam struts derived from polymer replica technique are as follows: (1) the natural hollow triangular channel and defects are generated during the polymer removal process; (2) the densification of SiC struts is usually difficult [4,5]. Many attempts have been reported in terms of solving the above two problems. Jun et al. [6] established the infiltration technique of immersing the pre-sintered foam green body into a ceramic slurry under a vacuum environment to smoothen the tips of the triangular holes and found that the compressive strength of the foams with improved macrostructure was two times higher than that of the untreated samples, whose value is 1.55 MPa with the porosity of 91%. Pu et al. [7] modified the polymer sponge templates with some chemical solutions in order to increase the solid content loading on the foam struts during the immersion process. Zhu et al. [8,9] focused on the slurry rheological behaviors and reported that SiC–Al_2O_3 foams presented a bending strength of 2.33 MPa with the porosity of 79%. Salazar [10] and Acchara [4] selected polymeric sponge templates with the different PPI (pores per inch) values separately. But due to its severely low mechanical strength of less than 1 MPa, no significant dependence of the macro cell sizes was observed. Therefore, the relationship between the macro cell sizes and the physical properties still remained undetermined experimentally.

Nowadays, liquid phase sintering of SiC foams has drawn worldwide attention [11–13], which can facilitate the

* Corresponding author. Tel.: +86 27 87217492; fax: +86 27 87879468.
E-mail address: chenfei027@gmail.com (Q. Shen).
[1] Member, the American Ceramic Society.

0272-8842/$36.00
doi:10.1016/j.ceramint.2012.03.030

densification and decrease the sintering temperature if appropriate sintering additives are chosen. These sintering additives include boron composites (such as B_4C and BN), aluminum and its composites (such as Al, Al_4C_3, AlN and Al_2O_3) and rare earth oxides (such as Y_2O_3 and La_2O_3). Up to now, the research work concerning SiC ceramic foams with high density of the cell strut via liquid phase sintering has been poorly achieved and no convincing densified microstructure has been reported. This paper will provide our latest experimental results of a highly densified cell strut with a systematic investigation of fabrication parameters, along with the control methods of structure and mechanical strength.

2. Experimental procedures

2.1. Starting materials

For preparation of SiC ceramic foams, the raw materials were chosen as follows: SiC powder (produced by Jiangyan Hanzhong Grinding Materials and Grinding Tools Co. Ltd., Jiangsu, China), Al_2O_3 powder (produced by Taimei Chemical Co. Ltd., Tokyo, Japan), Y_2O_3 powder (produced by Shanghai Chemical Reagent Research Institute, China). The average particle size of SiC powder is 3 μm, and that of other powders is 5 μm. The purity of all powders is 99.9%. Commercial polyurethane foams made from polyester polyol and methylene dichloride (produced by Changzhou Daye Tengfei Sponge Factory Co. Ltd., Jiangsu, China), whose complete pyrolysis temperature is 600 °C, were used as templates with the different PPI (pores per inch) values of 10, 15, 20 and 40, and the same dimensions of 20 mm × 20 mm × 10 mm. The silicone resin (Tianyuan Group Shanghai Resin Factory Co. Ltd., China) with the solvent of methylbenzene ($C_6H_5CH_3$) was selected as the binder, whose solid content is 55% and the viscosity is 8–35 mPa s at room temperature.

2.2. Preparation of SiC slurry

The ceramic powders of each composition series were mixed and blended uniformly with silicone resin to get the SiC slurry. SiC foams with no sintering additives were labeled as PURE SiC and those with Al_2O_3 and Y_2O_3 as sintering additives were labeled as SiC-AY. For series of SiC-AY, the oxides were added in the amount of 5 wt.%, 15 wt.% and 30 wt.%, which are marked as SiC-5AY, SiC-15AY and SiC-30AY, respectively. The molar ratio of Al_2O_3 and Y_2O_3 was fixed at 5:3 (equivalent to the weight ratio of 43:57), according to the lowest eutectic point of Al_2O_3 and Y_2O_3 at 1760 °C [14].

2.3. Preparation of SiC ceramic foams

After choosing the polymer sponge templates with the different PPI (pores per inch) values of 10, 15, 20 and 40, the experiment was carried out by immersing the polymer sponge templates into the ceramic slurry and then squeezed out the additional slurry in case of deteriorating the cell interconnection. The immersion and coating process was repeated for determination of coating time effect. Subsequently, the ceramic foams were dried at the room temperature and debonded at 600 °C at a heating rate of 0.2 °C/min, in order to remove the polymer and binder. Then the samples were sintered between 1400 and 1700 °C with a heating rate of 10 °C/min and different holding times, in a SiC powder bed in air and finally cooled naturally in the furnace to room temperature. A comparative experiment of sintering under Ar gas environment was also carried out.

2.4. Characterization

The density ρ of the foam material was calculated by weighing the mass and measuring the apparent volume. The density ρ_s of the ceramic strut solids was examined by Archimedes' method. According to the definition [15], the relative density of ceramic foams was ρ/ρ_s and the porosity was correspondingly $(1-\rho/\rho_s)$. The phase compositions were analyzed by X-ray diffraction (XRD) using a Rigaku Ultima III diffractometer (Japan). Cu radiation was used and operated at 40 kV and 40 mA and the scan rate of 10°/min was used to record the diffraction patterns in 2θ range between 10° and 80°. The microstructures of the cell size, cell struts and the fracture surface were observed by scanning electron microscopy (SEM) (Hitachi S-3400N, Japan). The compressive strength was investigated on a universal testing machine (MST 810, USA).

3. Results

3.1. Macrostructure of the SiC ceramic foams

Fig. 1 shows the typical macrostructure of SiC ceramic foam preforms with different PPI values after the first slurry coating and polymer removal step, among which the PPI values of (a), (b) and (c) are 10, 15 and 20, respectively. It is obvious that each of the SiC ceramic foam has uniform cell size, the identical strut diameter, good cell conductivity and almost no filled cells. Table 1 lists the macrostructure parameters, such as cell size and strut diameter, of SiC ceramic foam preforms with different PPI values.

Table 1
The macrostructure parameters of SiC ceramic foam preforms with different PPI values.

Polymer templates	Original diameter of the polymer templates	Strut diameter of the ceramic foam preforms	Macro size of the ceramic foam preforms
10PPI	340 μm	380 μm	2.20 mm
15PPI	230 μm	300 μm	1.90 mm
20PPI	200 μm	260 μm	1.40 mm

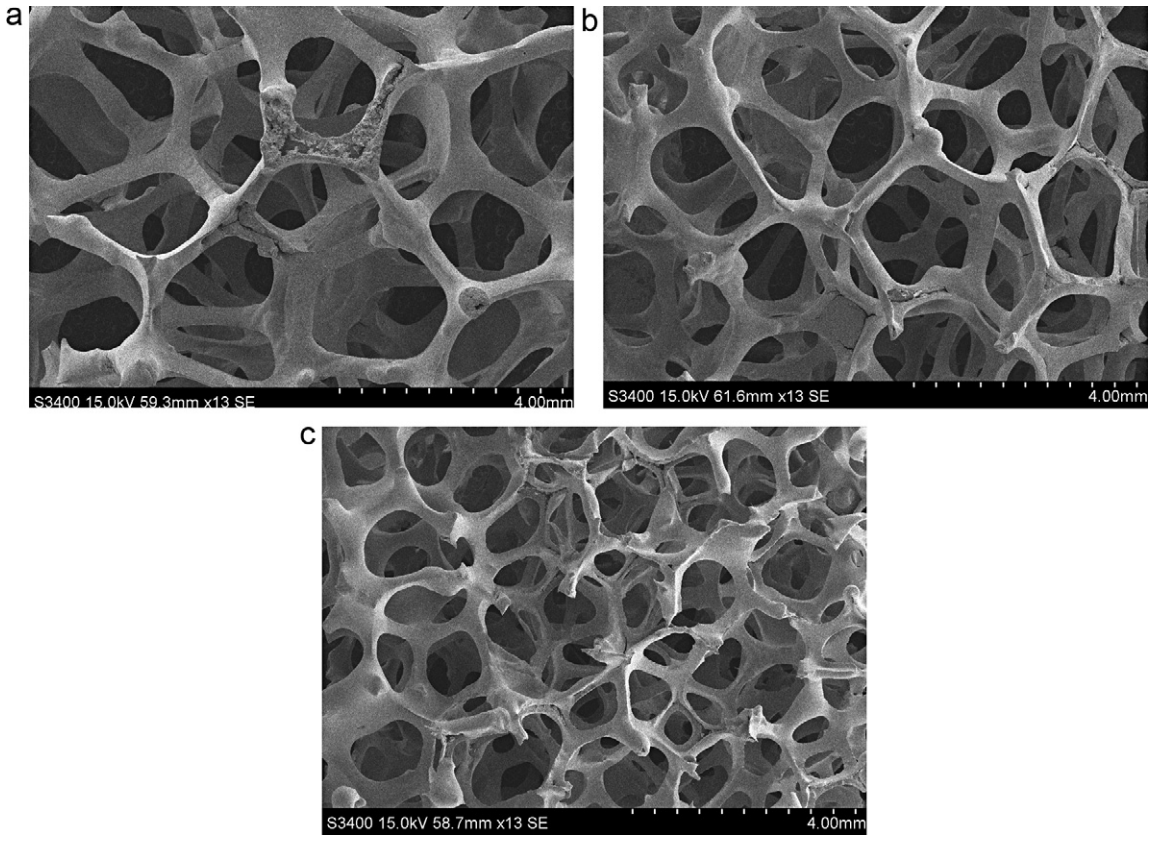

Fig. 1. Macrostructure of SiC ceramic foam preforms with different PPI values: (a) 10 PPI; (b) 15 PPI; (c) 20 PPI.

Fig. 2 shows the SiC ceramic foam strut diameters and porosity as a function of times of coating process. It can be seen from Fig. 2(a) that the strut diameters with the different PPI values exhibit a linear variation with the increase of the times of coating process. After the fifth coating, the strut diameter is increased from 340 μm to 690 μm compared with the initial one with PPI value of 10. As shown in Fig. 2(b), the porosity of ceramic foams steadily declines according to the increasing of coating process times, which is still in high range of porosity (more than 70%).

3.2. XRD analysis of the SiC ceramic foams

XRD is used to investigate the phase compositions of the raw powder and SiC ceramic foams with different chemical compositions (PURE SiC, SiC-5AY, SiC-15AY, SiC-30AY and SiC-30AY under Ar) with the identical sintering temperature of 1700 °C. It is clearly observed from Fig. 3 that the SiC phase is the dominant phase at every experimental condition. The intensities of SiC diffraction peak in all the testing samples remain unchanged before and after sintering at 1700 °C, suggesting the phase remains stable in the SiC ceramic foams. There is no obvious liquid phase detected in the samples of SiC-5AY and SiC-15AY. Only in the sample of SiC-30AY, liquid phase generates during high temperature sintering as a result of the sintering additives of Al_2O_3 and Y_2O_3, in the presence of $Y_3Al_5O_{12}$. However, with the same chemical composition, no liquid phase is detected in the sample of SiC-30AY under Ar environment.

Fig. 4 shows the different compositions of PURE SiC ceramic foams with different sintering temperatures. When the most noticeable reflections of SiC are kept at the same intensity with different conditions, the diffraction peak intensity of SiO_2 significantly declines with the increase of sintering temperatures, ranging from 1400 °C to 1600 °C. When the sintering temperature reaches 1600 °C, no SiO_2 phase is detected.

3.3. Microstructure of the SiC ceramic foams

Fig. 5 shows the effects of different sintering temperatures and chemical compositions with different sintering processes (PURE SiC, SiC-5AY, SiC-15AY and SiC-30AY) on the strut microstructures of SiC ceramic foams. While the macrostructure stays the same for all kinds of samples, as the characteristics of the triangle holes and channels; the close inspections of each strut fracture surface in Fig. 5(a)–(e) reveal great differences among them. During the polymer removal processed at lower debinding temperature of 600 °C, as is depicted in Fig. 5(a′), SiC powders of ceramic foam preforms only combine physically under the original binder adhesion in the SiC slurry. The foam itself undergoes almost no external forces and is easy to be collapsed under pressure. While during high temperature sintering, as is depicted in Fig. 5(b′)–(e′), SiC particles chemically coalesce by liquid phase sintering. However, different chemical compositions

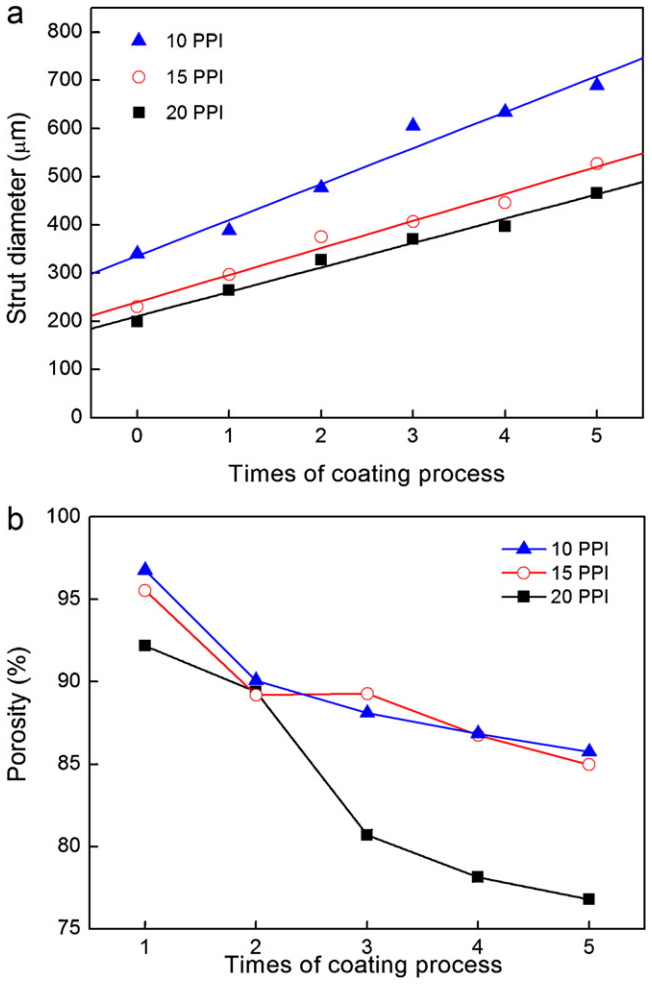

Fig. 2. Effect of times of coating process on (a) ceramic foam strut diameters and (b) ceramic foam porosity.

lead to considerable microstructure changes. In Fig. 5(b′) and (e′), at the same higher temperature sintering of 1700 °C, when there is no sintering additives of Al_2O_3 and Y_2O_3 as PURE SiC-1700 °C sample, the strut is full of micro-pores which degrades the mechanical strength. When the sintering additives are introduced, as depicted in Fig. 5(c′) and (d′), the cell strut begins to be compact with the sintered grains instead of being filled with pores and the densification degree is improved with the increase of sintering additive content. When the content of sintering additives reaches 30 wt.% as SiC-30AY-1700 °C sample, the cell strut densification is dramatically achieved with pore filling in Fig. 5(e′). The micro pores of cell struts are probably caused by the remaining interstices between particles with nothing movable filling in and may gradually be eliminated if the oxide reaction transformation from SiC to SiO_2 occurs. Only in Fig. 5(e′), the SiC grains are packed compactly and no micro-defect is observed. Thus, not all amount of sintering additives is competent for densification of foam cell struts. By adding Al_2O_3 and Y_2O_3 as the sintering additives and packed within the sintering powder, SiC foams, with uniform microstructure and densified struts, are obtained.

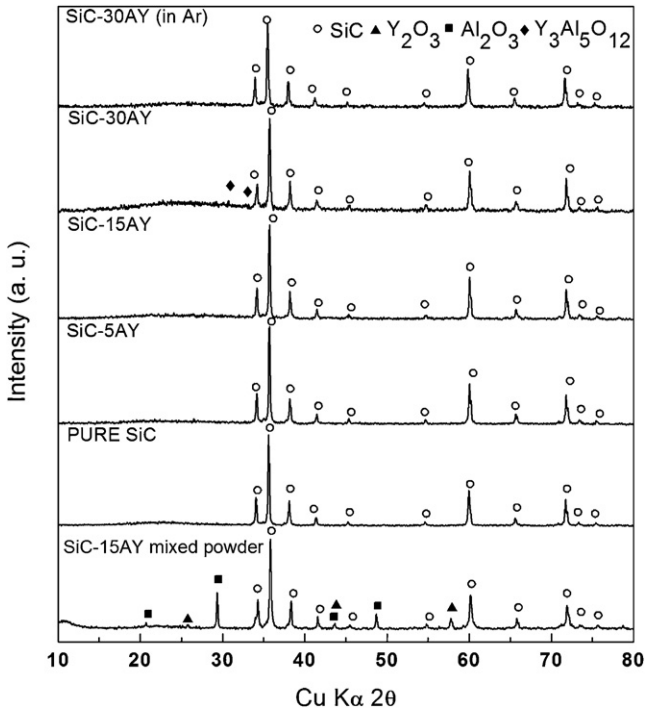

Fig. 3. XRD patterns of the raw powder and the ceramic foams with different chemical compositions and the same sintering temperature of 1700 °C.

3.4. Compressive strength of the SiC ceramic foams

Fig. 6 illustrates the scatter diagram of the compressive strength as a function of the relative density, while (a) refers to SiC ceramic foams with the same composition and different PPI values, and (b) refers to SiC ceramic foams with the same PPI value and different compositions. In Fig. 6(a), the greater the PPI values (or the smaller the cell sizes) of polymer templates are chosen, the higher the compressive strength presents, with the same relative density. The slight variance between the two samples of 20PPI-SiC-30AY probably was caused by different preparation and testing situations. In Fig. 6(b), comparing with the lowest strength of the sample of 20PPI-PURE-SiC, the sample of 20PPI-SiC-5AY presents the improvement in a small quantity of ~0.1 MPa. Then from SiC-15AY to SiC-30AY, the

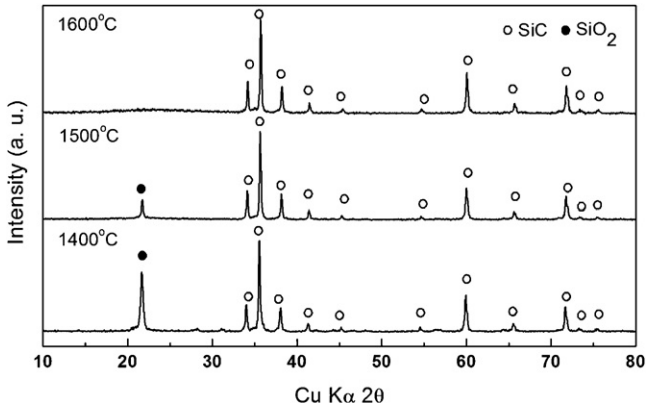

Fig. 4. XRD patterns of the PURE SiC ceramic foams with different sintering temperatures.

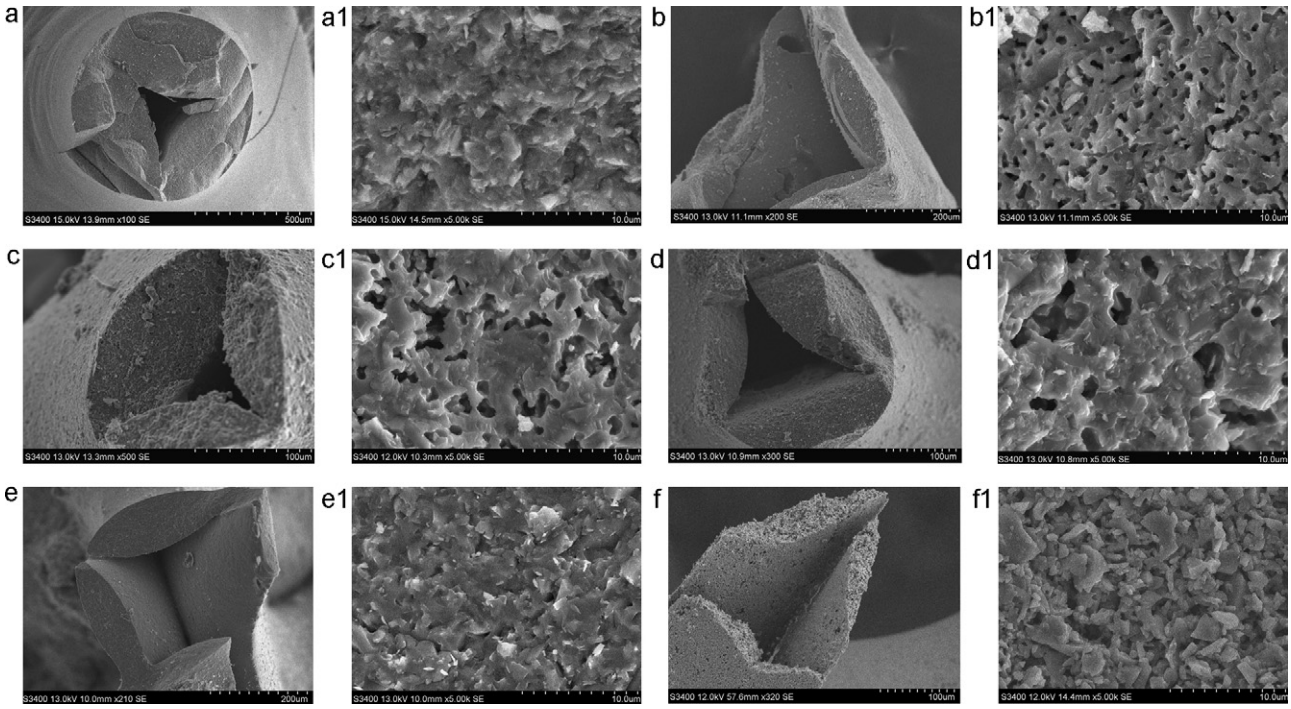

Fig. 5. Strut microstructures of SiC ceramic foams: (a) all samples heated after 600 °C, (b) PURE SiC-1700 °C, (c) SiC-5AY-1700 °C, (d) SiC-15AY-1700 °C and (e) SiC-30AY-1700 °C. Each magnification of the strut fracture surface is marked as (a′), (b′), (c′), (d′) and (e′).

scatters of the compressive strength distribute in the much higher numerical range with the same relative density of ∼20%, which is contributed to the corresponding increase in microstructure densification degree.

4. Discussion

4.1. Low temperature densification investigation of cell struts of SiC ceramic foams

The SiC oxidation behavior may attribute to the SiO_2 intensity change shown in Fig. 4. The high temperature oxidation mechanism of SiC includes two kinds of oxidation reactions: the passive oxidation ($SiC + 3/2O_2 = SiO_2 + CO$) and the active oxidation ($SiC + O_2 = SiO + CO$). The different behaviors of passive oxidation in which a silica protective layer is formed with a slight mass loss and active oxidation in which SiO_2 decomposes into SiO (g) with continuous weight loss can be transferred as a function of the partial oxygen pressure and the sintering temperature [16]. Thus, under low sintering temperatures, the presence of SiO_2 indicates the samples are still in the domain of passive oxidation. With the increase of the temperature, the critical transition for the passive to the active oxidation takes place and the SiO_2 phase on the surface of SiC is no longer stable. The evaporation of element silicon from the SiC results in the significant weight loss, leading to a homogenously distributed fine porosity in the microstructure. That can be proved according to the microscopic inspection of Fig. 5(b′). High temperature is responsible for the active oxidation domain, together with the achievement of sintering of SiC ceramics. Although passive oxidation occurs at relatively low temperatures with an outside silica layer to prevent the further oxidation, SiC ceramics cannot be completely sintered.

Liquid phase sintering of the samples packed with a SiC powder plays a significant role in the densification of the cell struts of SiC ceramic foams. In Fig. 3, the liquid phase $Y_3Al_5O_{12}$ in the sample SiC-15AY is generated during high temperature sintering as a result of the sintering additives, compared with no liquid phase of sample PURE SiC. Fig. 5 shows the effects of different sintering additives on the microstructure of the cell struts. The typical image of SiC active oxidation is the damaged surface with grain etching, such as the bubbles owning to the released gas of SiO or CO and crammed pits [16]. Those are partially in accordance with Fig. 5(b′)–(d′) because the damage of active oxidation with the protection of sintering bed is not as severe as those typical characteristics. The surrounding packed SiC powder can provide an equivalent partial pressure of the volatile species thus minimizing the appearance of the bubbles (SiO or CO), pits and the sharpened grains [17]. On the other hand, the more the sintering additive contents in the initial sample, the more the final liquid phase remains to heal the microscopic defects, as shown in Fig. 5(e′).

4.2. Effects of the macrostructure and microstructure on the mechanical property of the SiC ceramic foams

The use of polymeric templates with different PPI values can result in the controllable macrostructure of the SiC ceramic foams. While the cell shape and morphology are similar based on the characteristics of the open cell foam material, the templates with different PPI values can also cause changes in terms of not only the macrostructure parameters such as cell

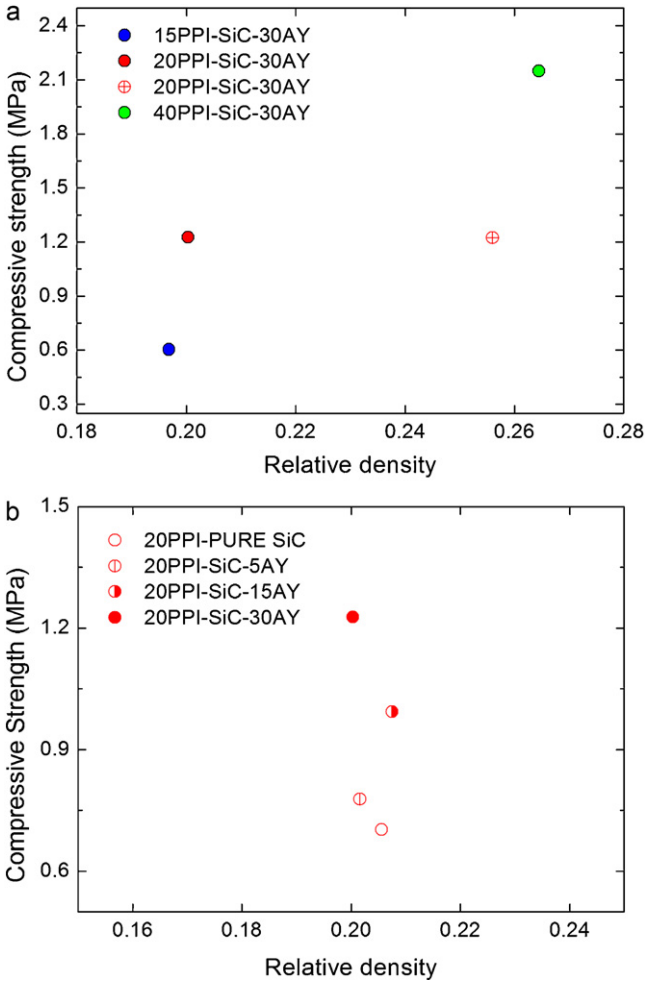

Fig. 6. Scatter diagram of compressive strength of SiC ceramic foams as a function of relative density: (a) SiC ceramic foams with the same composition and different PPI values; (b) SiC ceramic foams with the same PPI value and different compositions.

size and cell strut diameter, but also the porosity and relative density of the SiC ceramic foams. These are key factors determining the properties of cellular solids. It is generally accepted that the properties of cellular foams are dependent on their relative density [18]. Meanwhile, the strength of the foam material also depends on the structure of the individual foam strut.

It has been widely studied that different oxidation behaviors have different effects on the strength of SiC [19,20]. The strength of SiC may be improved in a short term by passive oxidation because the silica blunts the surface flaws, but may be reduced by active oxidation. The high weight loss during active oxidation leads to a decrease of the liquid phase content, limiting the solution-precipitation process, and finally reduces the densification process [19]. However, as discussed above, the microscopic defects can be healed due to the proper sintering additives and surrounding pack. The densification of SiC foam cell strut is not hindered when the SiC sintering bed is applied. Therefore, the densified cell struts of SiC ceramic foams can definitely improve the strength of the bulk material.

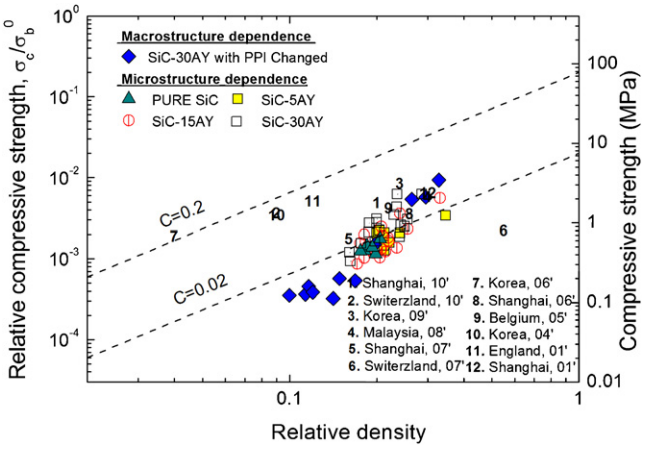

Fig. 7. Comparison of compressive strength of SiC ceramic foams as a function of relative density.

In order to make an intensive investigation of the effects of the macrostructure and microstructure on the compressive strength of SiC ceramic foams, the function of $\log(\sigma_c/\sigma_b^0)$ versus $\log(\rho/\rho_s)$ is plotted in Fig. 7, according to the theoretical formula $\sigma_c = C\sigma_b^0(\rho/\rho_s)^{3/2}$ [15] of cellular ceramics. The relative compressive strength is the ratio between the testing compressive strength σ_c of the SiC ceramic foams and the theoretical bending strength σ_b^0 of 450 MPa of SiC dense counterparts [2]. The compressive strength of our data as the colored spots is expected to increase with the increasing relative density. The numbers from 1 to 12 refer to those optimal properties reported in others' previous work from the year of 2001–2010 [5,6,11–13,21–27]. As can be seen, the value of C for open cell foams is 0.2 in the theoretical line with the slope of 3/2 [2,18] while the average value of C is only 0.02 in the fit of our data. It is noticeable that almost all the research results, including ours, present an obvious gap between the theoretical strength and the testing strength, owning to the inevitable macroscopic and microscopic defects (such as flaws, cracks, pores, bubbles, contamination, and impurities of grains) of the ceramic foams. The effect of microstructure on the mechanical property is clear based on our research. The PURE SiC, with an incomplete densified microstructure of the foam cell strut, shows the lowest compressive strength with the same PPI value of 20. And its C value may be less than 0.02. After the densification behavior of the samples is improved, e.g., in the samples of SiC-30AY, the strength increases obviously with the same relative density. Then, it is apparent that the C value increases close to 0.1 with this tendency of densification. It seems that the value of C can be one qualitative judgment of the densification degree in the microstructure of the SiC ceramic foams.

Consequently, we believe that the comprehensive effects of the macrostructure (namely the relative density) and microstructure (namely the densification of the cell struts) would both contribute to the enhancement of compressive strength. At the sintering temperature of 1700 °C, the compressive strength of SiC ceramic foams reaches the maximum value of 2.48 MPa with PPI value of 20 and the relative density of 77%.

5. Conclusions

(1) The macrostructure of SiC ceramic foams can be controlled by using different polymer sponge templates and altering the immersion and coating times. With the increase of the coating times, the ceramic strut diameter presents a linear increasing variation and the strut porosity is decreased.
(2) The microstructure of SiC ceramic foams can be controlled by adjusting the chemical compositions and sintering temperatures. SiC ceramic foams with highly densified struts are obtained when 30 wt.% Al_2O_3 and Y_2O_3 are used as sintering additives at the sintering temperature of 1700 °C.
(3) The comprehensive effects of the macrostructure and microstructure would both contribute to the enhancement of the compressive strength. After sintering at 1700 °C, the compressive strength of SiC ceramic foams reaches the maximum value of 2.48 MPa with PPI value of 20 and the relative density of 77%.

Acknowledgements

This work is supported by the National Natural Science Foundation of P. R. China under Grant No. 50972111, self-determined and innovative research funds of SKLWUT, and Research Fund of the Doctoral Program of Higher Education of China (No. 20110143110006).

References

[1] M.D.M. Innocentini, P. Sepulveda, V.R. Salvini, Permeability and structure of cellular ceramics: a comparison between two preparation techniques, J. Am. Ceram. Soc. 81 (1998) 3349–3352.
[2] A.R. Studart, U.T. Gonzenbach, E. Tervoort, Processing routes to macroporous ceramics: a review, J. Am. Ceram. Soc. 89 (2006) 1771–1789.
[3] P. Colombo, Conventional and novel processing methods for cellular ceramics, Philos. Trans. R. Soc. Lond. Ser. A 364 (2006) 109–124.
[4] W. Acchara, F.B.M. Souza, E.G. Ramalho, Mechanical characterization of cellular ceramics, Mater. Sci. Eng. A 513 (2009) 340–343.
[5] U.F. Vogt, M. Gorbar, P. Dimopoulos-Eggenschwiler, Improving the properties of ceramic foams by a vacuum infiltration process, J. Eur. Ceram. Soc. 30 (2010) 3005–3011.
[6] I.K. Jun, Y.M. Kong, S.H. Lee, H.E. Kim, H.W. Kim, K.C. Goretta, Reinforcement of a reticulated porous ceramic by a novel infiltration technique, J. Am. Ceram. Soc. 89 (2006) 2317–2319.
[7] X. Pu, L. Jia, D. Zhang, C. Su, X. Liu, Surface treatment of templates for fabrication of reticulated porous ceramics, J. Am. Ceram. Soc. 90 (2007) 2998–3000.
[8] X. Zhu, D. Jiang, S. Tan, Z. Zhang, Improvement in the strut thickness of reticulated porous ceramics, J. Am. Ceram. Soc. 84 (2001) 1654–1656.
[9] X. Zhu, D. Jiang, S. Tan, The control of slurry rheology in the processing of reticulated porous ceramics, Mater. Res. Bull. 37 (2002) 541–553.
[10] J.M.G. Salazar, M.I. Barrena, G. Morales, L. Matesanz, N. Merino, Compression strength and wear resistance of ceramic foams–polymer composites, Mater. Lett. 60 (2006) 1687–1692.
[11] X. Yao, S. Tan, X. Zhang, Z. Huang, D. Jiang, Low-temperature sintering of SiC reticulated porous ceramics with $MgO–Al_2O_3–SiO_2$ additives as sintering additives, J. Mater. Sci. 42 (2007) 4960–4966.
[12] U.F. Vogt, L. Gyorfy, A. Herzoga, T. Graule, G. Plesch, Macroporous silicon carbide foams for porous burner applications and catalyst supports, J. Phys. Chem. Solids 68 (2007) 1234–1239.
[13] R. Mouazer, S. Mullens, I. Thijs, J. Luyten, A. Buekenhoudt, Silicon carbide foams by polyurethane replica technique, Adv. Eng. Mater. 7 (2005) 1124–1128.
[14] J.H. She, K. Ueno, Effect of additive content on liquid-phase sintering on silicon carbide ceramics, Mater. Res. Bull. 34 (2009) 1629–1636.
[15] M.F. Ashby, R. Medalist, The mechanical properties of cellular solids, Metall. Trans. A 14 (1983) 1755–1769.
[16] L. Charpentier, M. Balat-Pichelin, F. Audubert, High temperature oxidation of SiC under helium with low-pressure oxygen. Part 1. Sintered α-SiC, J. Eur. Ceram. Soc. 30 (2010) 2653–2660.
[17] E.J. Winn, W.J. Clegg, Role of the powder bed in the densification of silicon carbide sintered with yttria and alumina additives, J. Am. Ceram. Soc. 82 (1999) 3466–3470.
[18] L.G. Gibson, M.F. Ashby, Cellular Solids Structure and Properties, Cambridge University Press, Cambridge, UK, 1997.
[19] G. Magnania, L. Beaulardib, L. Pilotti, Properties of liquid phase pressureless sintered silicon carbide obtained without sintering bed, J. Eur. Ceram. Soc. 25 (2005) 1619–1627.
[20] H. Kim, A.J. Moorhead, Effect of active oxidation on the flexural strength of α-silicon carbide, J. Am. Ceram. Soc. 73 (1990) 1868–1872.
[21] X. Yao, Z. Huang, S. Tan, Preparation of silicon carbide reticulated porous ceramics sintered at low temperature with PCS as sintering additive, J. Inorg. Mater. 25 (2010) 168–172.
[22] I.H. Jo, K.H. Shin, Y.M. Soon, Y.H. Koh, J.H. Lee, H.E. Kim, Highly porous hydroxyapatite scaffolds with elongated pores using stretched polymeric sponges as novel template, Mater. Lett. 63 (2009) 1702–1704.
[23] M. Nora, L.C. Hong, Z.A. Ahmad, H.M. Akil, Preparation and characterization of ceramic foam produced via polymeric foam replication method, J. Mater. Process. Technol. 207 (2008) 235–239.
[24] I.K. Jun, Y.H. Koh, J.H. Song, S.H. Lee, H.E. Kim, Improved compressive strength of reticulated porous zirconia using carbon coated polymeric sponge as novel template, Mater. Lett. 60 (2006) 2507–2510.
[25] X. Yao, S. Tan, Z. Huang, D. Jiang, Effect of recoating slurry viscosity on the properties of reticulated porous silicon carbide ceramics, Ceram. Int. 32 (2006) 137–142.
[26] M.R. Nangrejo, X. Bao, M.J. Edirisinghe, Processing of ceramic foams from polymeric precursor-alumina suspensions, Cell. Polym. 20 (2001) 17–36.
[27] X. Zhu, D. Jiang, S. Tan, Reaction bonding of open cell $SiC–Al_2O_3$ composites, Mater. Res. Bull. 36 (2001) 2003–2015.